Journal of Solid State Chemistry 182 (2009) 2239–2245

Contents lists available at ScienceDirect

Journal of Solid State Chemistry

journal homepage: www.elsevier.com/locate/jssc

Europium substitution into intermetallic phases grown in Ca/Zn flux

Milorad Stojanovic, Susan E. Latturner *

Department of Chemistry and Biochemistry, Florida State University, Tallahassee, FL 32306-4390, USA

ARTICLE INFO

Article history:
Received 3 March 2009
Received in revised form
21 May 2009
Accepted 1 June 2009
Available online 6 June 2009

Keywords:
Metal flux
Europium
Intermetallic
Nanostructuring

ABSTRACT

Replacement of calcium with europium in the phases $Ca_{21}Ni_2Zn_{36}$ and $CaNi_2Zn_3$ was attempted to explore the possibility of substitution in metal flux reactions and potential magnetic interactions between closely spaced Eu^{2+} ions. Limited substitution occurs when Eu is added to the reaction of nickel in a Ca/Zn flux mixture, up to stoichiometries of $Eu_{5.8(3)}Ca_{15.2(3)}Ni_2Zn_{36}$ and $Eu_{0.42(8)}Ca_{0.58(8)}Ni_2Zn_3$. Structural characterization and magnetic susceptibility studies on $Eu_xCa_{21-x}Ni_2Zn_{36}$ phases indicate that the Eu and Ca ions do not form an even solid solution on their sites, but instead segregate in separate regions of the crystals. The europium-rich regions of the samples order ferromagnetically, with T_C dependent on the size of the clusters. If the concentration of Eu in the flux is raised above 20 mol%, a new compound $Eu_{1.63(1)}Ca_{1.37(1)}Ni_2Zn_3$ (*Cmcm*, $a = 4.1150(5)$ Å, $b = 16.948(2)$ Å, $c = 10.302(1)$ Å, $Z = 4$, $R_1 = 0.0396$) is produced.

1. Introduction

A large number of investigations have shown that molten metal fluxes are a powerful tool in materials synthesis [1,2]. The solubility of many elements in molten metals renders them active at temperatures well below their melting point. Lower temperatures and the modified energetics in a flux allow for the isolation of different phases then those produced by traditional high temperature reactions [3]. Calcium metal is not considered promising as a flux due to its high melting point, volatility at high temperatures, and reactivity toward common crucible materials. Use of a calcium/zinc eutectic allows for synthesis at lower temperatures, which alleviates these problems. In previous work, the eutectic 7.3:2.7 molar ratio mixture of calcium and zinc metal which melts at 394 °C was explored as a solvent for the growth of new intermetallic compounds [4]. The reaction of nickel in this molten mixture produces two phases shown in Fig. 1—the $CaCu_5$ related structure $CaNi_2Zn_3$ (*P6/mmm*, $a = 8.9814(5)$ Å, $c = 4.0665(5)$ Å) and a new cubic structure $Ca_{21}Ni_2Zn_{36}$ (*Fd-3m*, $a = 21.5051(4)$ Å).

Given the large amount of calcium and short Ca–Ca distances in the $Ca_{21}Ni_2Zn_{36}$ structure, synthesis of a europium analog is of interest to investigate potential magnetic ordering. Europium is often divalent in intermetallic phases, and the ionic radii of this ion is similar to that of calcium (Ca^{2+} radius 1.00 Å; Eu^{2+} radius 1.17 Å) [5]. Unusual phenomena are possible in substituted intermetallics (spin glass behavior for randomly substituted materials, Kondo effects for mixed valent materials). Europium analogs of many calcium-containing polar intermetallic phases can be synthesized; fully substituted Eu analogs exist for $Ca_3Au_7Al_{26}Ti$ (orders ferromagnetically below 10 K), $BaAl_4$ analogs such as $CaPd_2Si_2$ (resulting in complex behavior caused by the presence of both Eu^{2+} and Eu^{3+}), and for many calcium-containing TiNiSi type intermetallics such as CaPdSn [6–8].

Using the Ca/Zn eutectic mixture as a synthesis medium, it was possible to partially substitute europium into both $Ca_{21}Ni_2Zn_{36}$ and $CaNi_2Zn_3$. The europium substitution on the calcium sites is not homogeneous across the $Eu_xCa_{21-x}Ni_2Zn_{36}$ phases; the calcium and europium ions appear to cluster in segregated regions of the crystals. This results in formation of ferromagnetic clusters of varying sizes, leading to unusual magnetic behavior. Attempts to increase the amount of Eu incorporation into the $Ca_{21}Ni_2Zn_{36}$ and $CaNi_2Zn_3$ structures yielded a compound with a new structure type. Similar attempts to substitute Yb^{2+} for Ca^{2+} led to formation of products with the complex CaCuAl structure type which is related to both $Ca_{21}Ni_2Zn_{36}$ and $CaNi_2Zn_3$.

2. Experimental procedure

Synthesis: Reactants were used as received: Ca shot (99.5%, Alfa Aesar), Zn granules (99.8%, Alfa Aesar), Ni powder (99.9%, Strem Chemicals), and Eu pieces (99%, Metall Rare Earth Ltd.). The initial reactant ratio which produced the two targeted phases was a 6:2:1 mmol ratio of Ca/Zn/Ni elements. Different amounts of europium were added to this mixture; see Table 1. The reactants were placed into stainless steel crucibles (7.0 cm length/0.5 cm diameter). An iron mesh filter was placed on top of each loaded

* Corresponding author. Fax: +1 850 644 8281.
E-mail address: latturne@chem.fsu.edu (S.E. Latturner).

0022-4596/$ - see front matter © 2009 Elsevier Inc. All rights reserved.
doi:10.1016/j.jssc.2009.06.001

crucible and held in place with a smaller alumina crucible. These were then placed in silica tubes which were sealed under vacuum. These ampoules were heated to 900 °C in 2 h and were kept at this temperature for 3 h. They were then cooled to 600 °C in 96 h, kept at 600 °C for 96 h, and cooled to 450 °C in 48 h; at this temperature, the tubes were removed from the furnace, inverted, and centrifuged to force the excess molten Ca/Zn eutectic through the filter. The solid product remaining in the crucibles consisted of small shiny gray and gold—tinged metallic crystals. The gray crystals (hexagonal phase) are air stable and very brittle. The gold—tinged crystals (cubic phase) are not as brittle and they develop an oxide coating if left exposed to air for longer than a week.

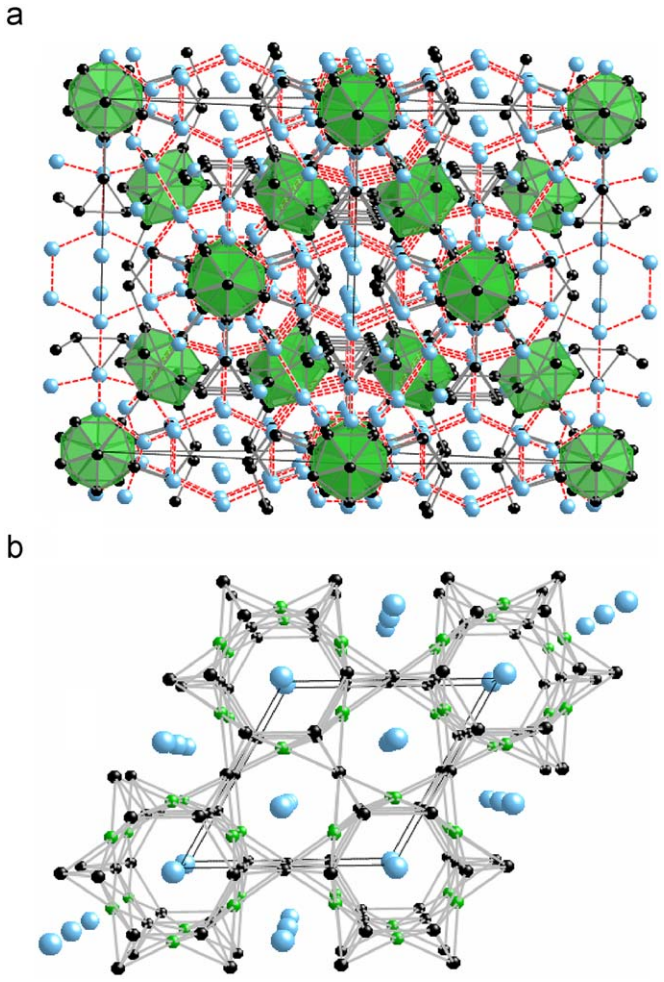

Fig. 1. The structures of: (a) $Ca_{21}Ni_2Zn_{36}$ and (b) $CaNi_2Zn_3$. Blue spheres are calcium atoms, green spheres are nickel, and black spheres are zinc. The short distances between calcium sites in the former structure are highlighted by red dashed lines, and the icosahedral coordination of the nickel site is shown as green polyhedra. (For interpretation of the references to color in this figure legend, the reader is referred to the web version of this article.)

In previous studies of Ca/Zn/Ni reactions, excess flux was dissolved by soaking the product in water [4]. However, the Eu-containing phases in this study are far more sensitive to degradation in water and air than their calcium analogs; centrifugation is vital to avoiding decomposition. Also, residual flux coating was minimized by centrifugation; this allows the product phases to be more easily visually distinguished, and improves the accuracy of the elemental analysis. Finally, binary phases such as $CaZn_2$, which form if the flux is allowed to cool to room temperature, are no longer present since the centrifuging takes place above the temperature of their precipitation.

Elemental analysis: Samples from each reaction were affixed to an aluminum SEM stub using carbon tape. Elemental analysis was performed using a JEOL 5900 scanning electron microscope with energy dispersive spectroscopy (EDS) capabilities. Samples were analyzed using a 30 kV accelerating voltage and an accumulation time of 60 s. Internal regions of cracked crystals were analyzed to avoid traces of residual flux coating the surface. The average *R* (sum of Ca and Eu):Ni:Zn molar percentage seen for the cubic phase is *R* 30%, Ni 5% and Zn 55%. The average ratio of the hexagonal phase is *R* 20%, Ni 30% and Zn 50%, making the two phases easily distinguishable using EDS.

X-ray diffraction: Small spheroid pieces from the larger crystals analyzed using EDS were mounted on glass fibers with epoxy. Single crystal X-ray diffraction data was collected at room temperature using a Bruker AXS SMART CCD diffractometer with a Mo radiation source. Processing of the data was accomplished with use of the program SAINT; an absorption correction was applied to the data using the SADABS program. Refinement of the structure was performed using the SHELXTL package [9]. Nickel and zinc sites are in many cases distinguishable in the X-ray data despite their similar electron density; assignments agreed with bond length arguments, comparison with previously published structures, and elemental analysis. Crystallographic information for several of the compounds studied here can be found in Tables 2 and 3. Further details of the crystal structure investigations can be obtained from the Fachinformationszentrum Karlsruhe, 76344 Eggenstein-Leopoldshafen, Germany (fax: +49 7247 808 666; e-mail crysdata@fiz.karlsruhe.de) on quoting the depository

Table 1
Europium substitution in $Ca_{21}Ni_2Zn_{36}$ and $CaNi_2Zn_3$.

Reaction ratio Ca:Zn:Ni:Eu	Formula	Unit cell parameters (Å)		R_1[a]
$Eu_xCa_{21-x}Ni_2Zn_{36}$		*a*		
6:2:1	$Ca_{21}Ni_2Zn_{36}$	21.5051(4)		0.0494
6:2:1:0.5	$Eu_{2.4(7)}Ca_{18.6(7)}Ni_2Zn_{36}$	21.5683(11)		0.0210
6:2:1:1.5	$Eu_{4.0(2)}Ca_{17.0(2)}Ni_2Zn_{36}$	21.5814(11)		0.0983
6:2:1:2	$Eu_{5.8(3)}Ca_{15.2(3)}Ni_2Zn_{36}$	21.7557(6)		0.0811
$Eu_xCa_{1-x}Ni_2Zn_3$		*a*	*c*	
6:2:1	$CaNi_2Zn_3$	8.9814(5)	4.0665(5)	0.0246
6:2:1:0.2	$Eu_{0.05(6)}Ca_{0.95(6)}Ni_2Zn_3$	8.9855(8)	4.0604(8)	0.0316
6:2:1:0.4	$Eu_{0.1(1)}Ca_{0.9(1)}Ni_2Zn_3$	9.0368(9)	4.0864(8)	0.0551
6:2:1:0.75	$Eu_{0.19(4)}Ca_{0.81(4)}Ni_2Zn_3$	9.0128(4)	4.0767(4)	0.0231
6:2:1:1	$Eu_{0.25(8)}Ca_{0.75(8)}Ni_2Zn_3$	9.0165(6)	4.0737(5)	0.0353
6:2:1:1.25	$Eu_{0.3(1)}Ca_{0.7(1)}Ni_2Zn_3$	9.0182(26)	4.0709(24)	0.0457
6:2:1:2	$Eu_{0.42(5)}Ca_{0.58(5)}Ni_2Zn_3$	9.0119(45)	4.0747(42)	0.0217

[a] R_1 [$I > 2\sigma(I)$].

Table 2
Crystallographic data collection parameters for representative Eu/Ca/Ni/Zn phases.

Parameter	$Eu_{2.4(7)}Ca_{18.6(7)}Ni_2Zn_{36}$	$Eu_{0.25(8)}Ca_{0.75(8)}Ni_2Zn_3$	$Eu_{1.63(1)}Ca_{1.37(1)}Ni_2Zn_3$
Formula weight (g/mol)	3581.28	381.57	612.76
Space group	*Fd*-3*m*	*P*6/*mmm*	*Cmcm*
a (Å)	21.568(1)	9.0165(6)	4.1150(5)
b (Å)			16.948(2)
c (Å)		4.0737(5)	10.302(1)
V (Å^3)	10033.4(1)	286.8(1)	718.4(2)
δ_{calc} (g/cm^3)	4.754	6.628	5.664
Z	8	3	4
Temperature (K)	298	298	298
Radiation	Mo *K*α	Mo *K*α	Mo *K*α
Index ranges	$-28 \le h,k,l \le 28$	$-12 \le h \le 12$ $-11 \le k \le 11$ $-5 \le l \le 5$	$-5 \le h \le 5$ $-22 \le k \le 22$ $-13 \le l \le 13$
Absorption coeff. (mm^{-1})	22.48	24.45	29.60
Reflections collected	34641	3558	4864
Unique data/parameters	647/39	177/19	533/33
R_1/wR_2 ($I > 2\sigma(I)$)	0.0210/0.0519	0.0353/0.0693	0.0397/0.0880
Residual peak/hole (e$^-$ Å^{-3})	0.62/−0.79	1.78/−1.54	1.35/−2.13

Table 3
Atomic positions and thermal parameters for $Eu_{1.63}Ca_{1.37}Ni_2Zn_{3-\delta}$.

Atom	Wyckoff site	*x*	*y*	*z*	Occupancy	U_{eq}[a]
Eu_1/Ca_1	8*f*	0	0.34579(5)	0.44410(9)	0.576(6)/0.424(6)	0.0168(3)
Eu_2/Ca_2	4*c*	0	0.12023(8)	$\frac{1}{4}$	0.481(4)/0.519(4)	0.0146(5)
Ni_1	8*f*	0	0.49264(8)	0.6312(1)	1	0.0117(4)
Zn_1	4*a*	0	0	$\frac{1}{2}$	1	0.0134(4)
Zn_2	4*c*	$\frac{1}{2}$	0.4419(1)	$\frac{1}{4}$	1	0.0169(5)
Zn_3	4*c*	0	0.2346(1)	$\frac{3}{4}$	0.93(1)	0.0229(8)

[a] U_{eq} is defined as the trace of the orthogonalized U_{ij} tensor.

numbers CSD 420706 through 420709. Powder X-ray diffraction data were collected with a Rigaku Ultima III Powder X-ray Diffractometer; a small amount of silicon was added to act as an internal standard. The unit cell parameters were refined using the accompanying MDI Jade software package.

Magnetic susceptibility: Sample crystals of the Eu/Ca/Ni/Zn phases were first screened using EDS. For each phase being studied, several crystals were weighed and sealed into a piece of kapton tape. Magnetic measurements were carried out with a Quantum Design MPMS SQUID magnetometer at temperatures between 2 and 300 K. Temperature-dependent susceptibility data were collected at fields between 500 and 20 000 G, and field dependence data were collected at several temperatures.

3. Results and discussion

Three phases are produced when europium metal is added to Ca/Zn/Ni reactions: europium-doped $CaNi_2Zn_3$ and $Ca_{21}Ni_2Zn_{36}$, and $Eu_{1.63}Ca_{1.37}Ni_2Zn_3$, a phase which cannot be isolated as a pure calcium phase. The first phase is predominant in reactions with lower europium amounts added (a 6:2:1:0.5 mmol Ca/Zn/Ni/Eu reaction yields 75% $Eu_xCa_{1-x}Ni_2Zn_3$ type); higher concentrations of Eu yield more of the second phase (6:2:1:2 mmol ratio products are 60% $Eu_xCa_{21-x}Ni_2Zn_{36}$ type). The overall yields are somewhat less than those reported for the pure calcium phases [4]. The third phase ($Eu_{1.63}Ca_{1.37}Ni_2Zn_3$) is not formed unless at least 2.25 mmol of europium are present in the reaction. Europium-substituted compounds are not as air stable as the Ca/Ni/Zn ternary phases, degrading after about a week depending on the amount of europium that is incorporated. All products were therefore stored in a dry box under argon. Reactions in the Eu/Zn eutectic (75 mol% Eu, melting point 510 °C) were investigated to see if pure europium variants could be synthesized. Unfortunately, no ternary phases were isolated. The $EuZn_2$ phase is difficult to avoid in this reaction system; this, combined with the expense of this flux, limits its utility. Stoichiometric synthesis also failed to yield europium analogs.

$Eu_xCa_{21-x}Ni_2Zn_{36}$: The cubic $Ca_{21}Ni_2Zn_{36}$ structure was of particular interest for doping with magnetic elements. Of the four crystallographic calcium sites in the unit cell, three are within 3.5 Å of a neighboring Ca site; these short distances are denoted by the dashed red lines in Fig. 1a. This distance is in the vicinity of the Hill limit (3.4–3.5 Å) below which direct coupling between rare earth ions substituted onto the sites becomes possible [10]. The calcium site occupancies determined from single crystal XRD studies of several $Eu_xCa_{21-x}Ni_2Zn_{36}$ products indicate that europium substitutes on all four calcium sites; there is no evidence of europium preferring a specific site. The maximum amount of europium incorporation observed in this phase is 28%, resulting in a stoichiometry of $Eu_{5.8(3)}Ca_{15.2(3)}Ni_2Zn_{36}$. Higher amounts of europium added to the Ca/Zn/Ni mixture did not increase the Eu content of this phase, indicating a limit to the solid solution range of this compound. The ordering of Ni and Zn on their respective crystallographic sites is identical to that in the $Ca_{21}Ni_2Zn_{36}$ parent structure [4].

Comparison of unit cell parameters from both single crystal and powder data reveals that this system does not obey Vegard's law (Table 1). High *R*(int) and R_1 values for the data sets of the more Eu-rich phases indicate that the single crystals contain defects. Although twinning was problematic in some cases, it was not always present, indicating the quality problem with these materials is a more subtle kind of disorder. These characteristics may be the result of clustering of europium in the crystals. Instead of being evenly distributed on the calcium sites as a solid solution, it appears that there are local regions in the crystals that are europium-rich. The growth of such segregated nanostructures within the crystals may result in poor diffraction data, since diffraction is a long-range averaging technique.

Segregation of different cations in separate regions of a solid has been observed in other systems. For instance, an attempted gallium flux growth of the clathrate solid solution $Ba_xSr_{8-x}Ga_{16}Ge_{30}$ lead to core-shell single crystals that were predominantly $Ba_8Ga_{16}Ge_{30}$ in the center and $Sr_8Ga_{16}Ge_{30}$ on the outer surface [11]. Similarly, attempted synthesis of the clathrate

$Eu_2Ba_6Al_{16}Si_{30}$ led to a sample that appears to have segregated into europium- and barium-rich clathrate regions. The inhomogeneity of the sample was not discernable by powder XRD due to very similar unit cell parameters of the phases [12]. Control of this process is of great interest for the modification of materials properties—deliberate "nanostructuring" of thermoelectric materials has lead to vastly improved Seebeck coefficients in the $AgPb_mSbTe_{m+2}$ system, for example [13]. Synthesis technique may play a major role in causing segregation of elements. Flux synthesis allows for isolation of compounds with clustering of Eu; annealing at high temperatures might promote formation of a more evenly distributed solid solution.

Magnetic properties of $Eu_xCa_{21-x}Ni_2Zn_{36}$: The inhomogeneous distribution of europium in $Eu_xCa_{21-x}Ni_2Zn_{36}$ is also indicated by the magnetic properties of the compounds. The magnetic susceptibility temperature dependence data for three samples is shown in Fig. 2. At high temperatures, the compounds are paramagnetic and the fit of the data to the Curie–Weiss law (using data from 100 to 300 K) indicates a magnetic moment per europium ion between 7.5 and 8.5μ_B for all samples, in agreement with the expected value of 7.94μ_B for Eu^{2+} ions. For the more air-sensitive $Eu_{5.8}Ca_{15.2}Ni_2Zn_{36}$ analog a slight curvature is seen near 75 K, likely due to formation of a small amount of surface EuO (which has a ferromagnetic transition at 70 K). At low temperatures, deviations from Curie–Weiss behavior indicate interactions between the europium spins. A solid solution with an even, random distribution of Eu^{2+} across the sample might be expected to show spin glass behavior, depending on concentration. This is not observed—the field cooled and zero-field cooled susceptibility data are identical, and AC susceptibility measurements did not show any frequency dependence for the data. What is seen is a ferromagnetic transition, with a T_C that increases with europium content. The segregated regions of "$Eu_{21}Ni_2Zn_{36}$" will increase in size with more europium incorporation, and the strength of the ferromagnetic coupling increases as the number of spins rises. As the europium-rich clusters grow in size, the ferromagnetic ordering temperature rises from a T_C of 25 K for $Eu_{2.4}Ca_{18.6}Ni_2Zn_{36}$, to a T_C of 40 K for $Eu_{4.0}Ca_{17.0}Ni_2Zn_{36}$, and finally to a T_C of 60 K for $Eu_{5.8}Ca_{15.2}Ni_2Zn_{36}$. In agreement with this trend, the Weiss constants derived from the Curie–Weiss fit of the high temperature data for these phases are $\theta = 17$, 27, and 33 K, respectively.

Similar variations in magnetic ordering temperature with stoichiometry have been observed in studies of YFe_xAl_{12-x} systems; the observed T_C is dependent on iron content. Structural characterization indicates that the iron atoms preferentially occupy the 8*f* and 8*j* sites of the $ThMn_{12}$-type structure. However, the magnetic susceptibility behavior reveals that the iron in these phases is not distributed evenly across the sample, but instead forms iron-rich regions that order ferromagnetically. Mössbauer and AC susceptibility studies also indicate the presence of Fe-rich clusters in these materials [14].

Magnetization data for the $Eu_{5.8(3)}Ca_{15.2(3)}Ni_2Zn_{36}$ sample taken at several temperatures is shown in Fig. 3. Data taken above T_C (60 K for this compound) are linear, indicative of paramagnetism. Below the ordering temperature, signs of the ferromagnetic coupling are observed, although the lack of hysteresis indicates the europium-rich regions are soft ferromagnets. Saturation is approached below the theoretical value expected for the europium content of the compound, supporting the model of segregated regions exhibiting ferromagnetic order instead of the entire sample.

$Eu_xCa_{1-x}Ni_2Zn_3$: This structure type (Fig. 1b) has two crystallographic calcium sites onto which europium can substitute. The europium dopes both sites approximately equally; the highest amount of europium substitution is 42 mol% (Table 1). Unlike the more Ca/Eu-rich cubic phases, these $Eu_xCa_{1-x}Ni_2Zn_3$ compounds are air stable for long periods of time. Magnetic susceptibility measurements on several of these samples show paramagnetic behavior of Eu^{2+} ions with no indication of magnetic ordering down to 2 K. This is understandable given the larger separation

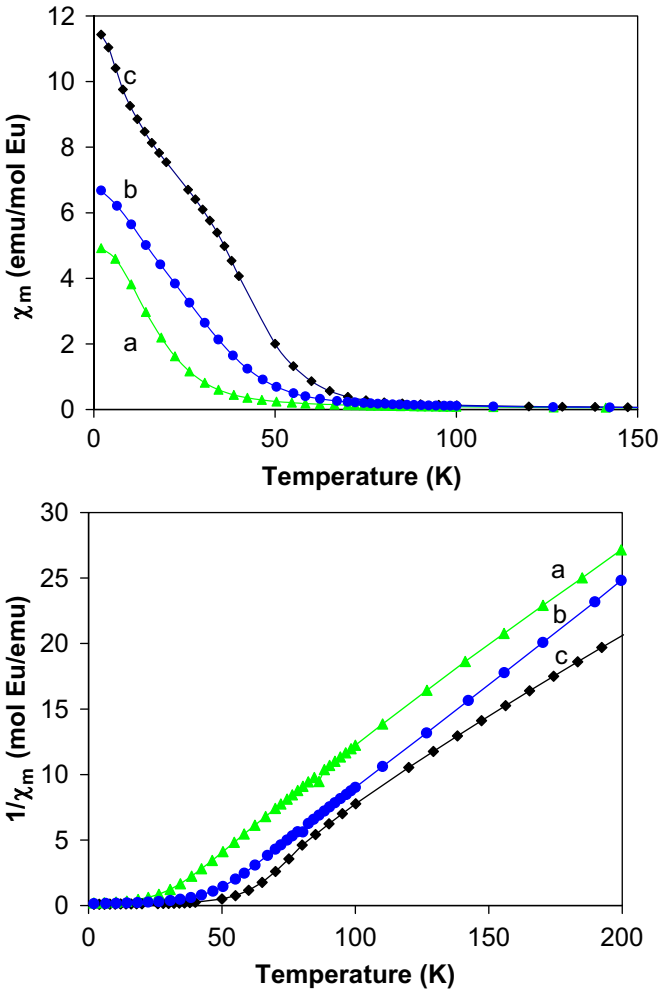

Fig. 2. Magnetic molar susceptibility and inverse susceptibility of $(Ca/Eu)_{21}Ni_2Zn_{36}$ phases at different Eu substitution levels: (a) $Eu_{2.4(7)}Ca_{18.6(7)}Ni_2Zn_{36}$; (b) $Eu_{4.0(2)}Ca_{17.0(2)}Ni_2Zn_{36}$; and (c) $Eu_{5.8(3)}Ca_{15.2(3)}Ni_2Zn_{36}$.

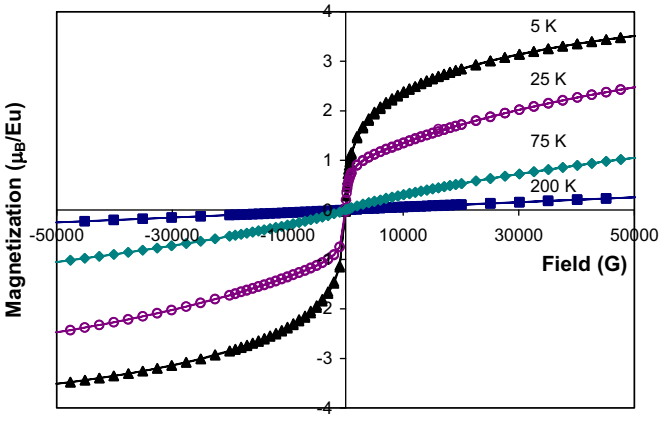

Fig. 3. Field dependence of the magnetization of $Eu_{5.8(3)}Ca_{15.2(3)}Ni_2Zn_{36}$ at temperatures above and below the ordering temperature ($T_C = 60$ K).

between Ca/Eu sites in this structure (over 4 Å) compared to the cubic structure.

$Eu_{1.63}Ca_{1.37}Ni_2Zn_3$: This compound was produced in syntheses aimed at making more europium-rich $Eu_xCa_{21-x}Ni_2Zn_{36}$ compounds. It does not exist as a pure calcium phase and forms only in reactions containing over 20 mol% europium. It is the europium richest phase isolated in these syntheses; the two Eu/Ca sites contain 54% europium and 46% calcium on the two crystallographic Eu/Ca sites. Different reaction stoichiometries produce identical Eu:Ca ratios in this structure, indicating that it may be a line compound or that it exists in a very small phase width. The compound is air sensitive and decomposes after couple of days in air.

$Eu_{1.63}Ca_{1.37}Ni_2Zn_3$ has a new orthorhombic structure type, shown in Fig. 4. It features puckered sheets of nickel and zinc atoms which are separated by layers of Eu/Ca mixed sites. The sites in this sheet were originally refined as zinc, but when the occupancies were allowed to vary, the 8*f* site had $<100\%$ occupancy. This site features a short bond distance (2.448(3) Å) to its symmetry equivalent and was therefore assigned as nickel (see Table 3). Assignment was more difficult for the relatively isolated Zn_3 sites within the Eu/Ca layer. Multiple crystals of this phase were studied using XRD and this site is partially occupied in all of the structure solutions, whether it is assigned as Ni (96% occupied) or Zn (93% occupied). It was assigned as zinc based on observed bond lengths and elemental analysis. These Zn_3 atoms reside in a trigonal prism of Eu/Ca atoms (Zn–Eu/Ca distances range from 3.15(6) to 3.21(2) Å) and they are 2.99(3) Å from the apical Zn of the puckered nickel/zinc sheet. The partial occupancy results in a stoichiometry of $Eu_{1.63(1)}Ca_{1.37(1)}Ni_2Zn_{2.9(1)}$; since the deviation from full occupancy is small, the formula $Eu_{1.63}Ca_{1.37}Ni_2Zn_3$ is used for simplicity.

This compound has a higher ratio of highly electropositive metal (Ca/Eu) to more electronegative metals (Ni/Zn) than the two structures shown in Fig. 1. This favors the conversion from the 3-D networks of nickel and zinc encapsulating the Ca or Eu atoms (observed in the $CaNi_2Zn_3$ and $Ca_{21}Ni_2Zn_{36}$ structures) to a 2-D structure with a Ni/Zn sheet separated by layers of Ca/Eu in the $Eu_{1.63}Ca_{1.37}Ni_2Zn_3$ phase. Other Ca/M/Zn phases grown in Ca/Zn flux show a similar relationship between transition metal bonding topology and calcium content. CaPdZn has a 1:2 ratio of calcium to transition metal atom and a 3-D network of palladium and zinc (in the TiNiSi structure type); $Ca_6Pt_3Zn_5$ has a 3:4 ratio of Ca:TM and features a 2-D puckered sheet of transition metals (in a modification of the W_3CoB_3 structure type) [4]. This reduction of dimensionality with increasing alkaline earth content mirrors the behavior of Zintl phases, which have main group element building blocks that decrease in dimensionality as the amount of alkali metal/alkaline earth metal increases. For instance, Na_8Sn_{44} has a 3-D network of tin encapsulating sodium ions in the cages; $A_3Na_{10}Sn_{23}$ (A = Cs, Rb, K) has a layered structure; and Na_4Sn_4 has 0-D clusters of Sn_4^{4-} surrounded by Na^+ ions [15]. Another factor comparable to the behavior of Zintl phases is the importance of different cations in directing the structure. $A_3Na_{10}Sn_{23}$ and $A_8Na_{16}Ge_{136}$ (A = Cs, Rb) are both stabilized by the presence of two different alkali metals [16]. The lack of a pure calcium analog of $Eu_{1.63}Ca_{1.37}Ni_2Zn_3$ and the narrow phase width may indicate that a specific mixture of Eu and Ca is required for the stabilization of this structure.

Magnetic properties of $Eu_{1.63}Ca_{1.37}Ni_2Zn_3$: The two Eu/Ca mixed sites in this structure appear to produce complex magnetic behavior, as shown in Fig. 5. Despite the fact that samples were stored and handled in a glove box, a small amount of surface EuO readily forms, evidenced by clear signs of a ferromagnetic transition at 70 K. Susceptibility data was therefore collected at high fields (30 000 G) to saturate the ferromagnetic signal of this impurity. The resulting high temperature inverse susceptibility data (above 150 K) is linear and can be fit to the Curie–Weiss law, producing a magnetic moment per europium ion of $8.0\mu_B$. The negative Weiss constant ($\theta = -41.3$ K) indicates antiferromagnetic

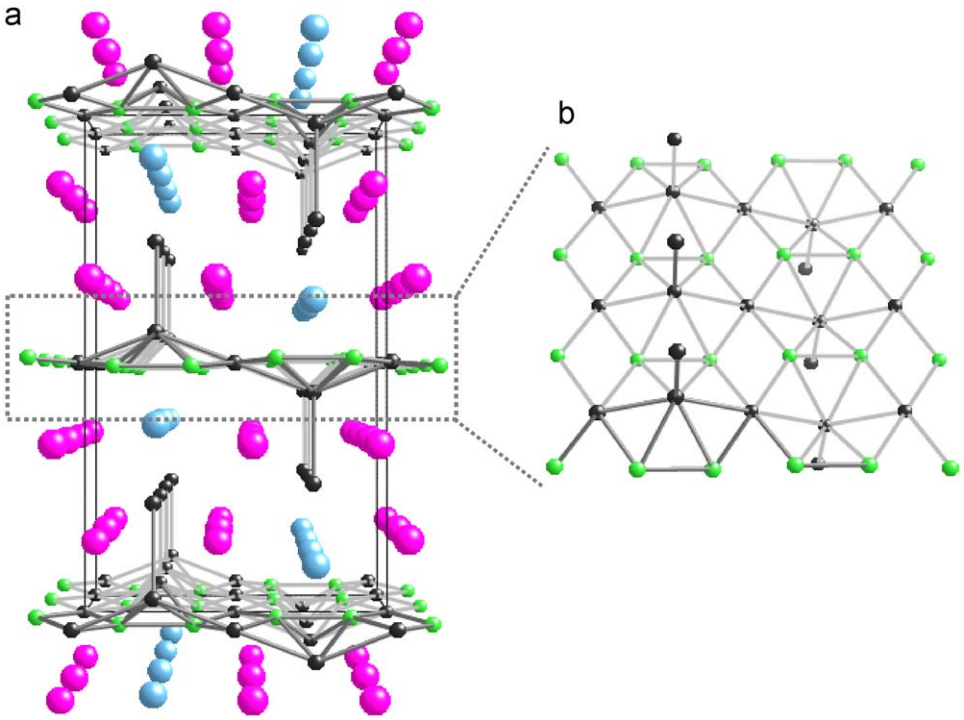

Fig. 4. The structure of $Eu_{1.63}Ca_{1.37}Ni_2Zn_3$. Blue spheres represent the Ca-rich 4*c* site; pink spheres represent the Eu-rich 8*f* site: (a) unit cell viewed down the *a* axis and (b) view of the puckered Ni/Zn sheet, viewed down the *b* axis. (For interpretation of the references to color in this figure legend, the reader is referred to the web version of this article.)

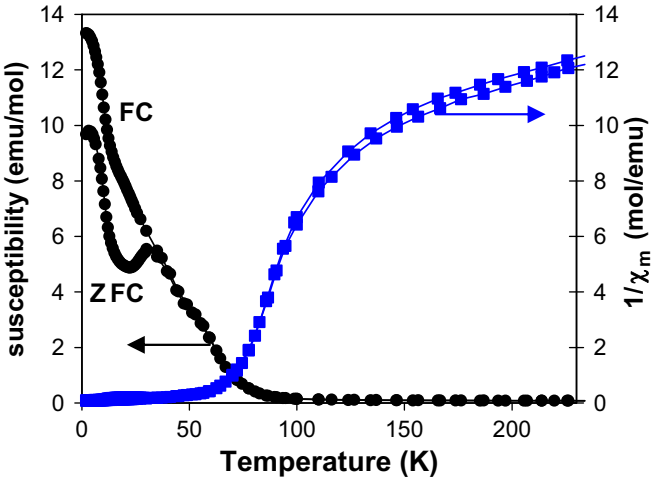

Fig. 5. Temperature dependence of the magnetic susceptibility and inverse susceptibility of $Eu_{1.63}Ca_{1.37}Ni_2Zn_3$ at 500 G, showing the deviation of zero-field cooled and field cooled behavior below the ordering transition at 30 K.

coupling between the magnetic ions. Data collection at low fields was carried out to observe any magnetic transitions that might be overwhelmed at higher fields. Antiferromagnetic ordering is indicated by the cusp at 30 K observed in the susceptibility data collected at 500 G (see Fig. 5). It is notable that the field-cooled and zero-field cooled data diverge at this point, which is a common sign of spin glass behavior [17]. AC susceptibility studies are needed to further investigate this.

Attempts at ytterbium substitution: Like europium, ytterbium is often divalent in intermetallics and can substitute for calcium. Substitution was attempted by adding Yb metal into Ca/Zn/Ni synthesis mixtures. However, very little Yb incorporation was seen in the $CaNi_2Zn_3$ and $Ca_{21}Ni_2Zn_{36}$ products, with a maximum of 9% and 1% substitution, respectively. The majority of the Yb was instead found in the products $YbZn_2$ and $Yb_{6.7+x}Ca_{24.7-y}Ni_9Zn_{54}$. The latter phase is an analog of the CaCuAl structure type [18]. The hexagonal structure (shown in Fig. 6; additional crystallographic information in Supplementary Data) is highly complex and shows similar bonding motifs to both the $Ca_{21}Ni_2Zn_{36}$ and $CaNi_2Zn_3$ structures. As in $Ca_{21}Ni_2Zn_{36}$, it features a nickel site surrounded by twelve zinc atoms in an icosahedral coordination sphere, and this icosahedron is surrounded by Ca/Yb mixed sites in the configuration of a pentagonal dodecahedron (see Fig. 6b). Like $CaNi_2Zn_3$, a chain of Ca/Yb sites runs along the *c* axis and is surrounded by a hexagonal channel of nickel and zinc atoms (Fig. 6c). These similarities were used to aid in the assignment of nickel and zinc sites; bond lengths and elemental analysis were also considered. Nonetheless, distinction between these two elements is difficult using XRD and it is possible that Ni/Zn site mixing may occur.

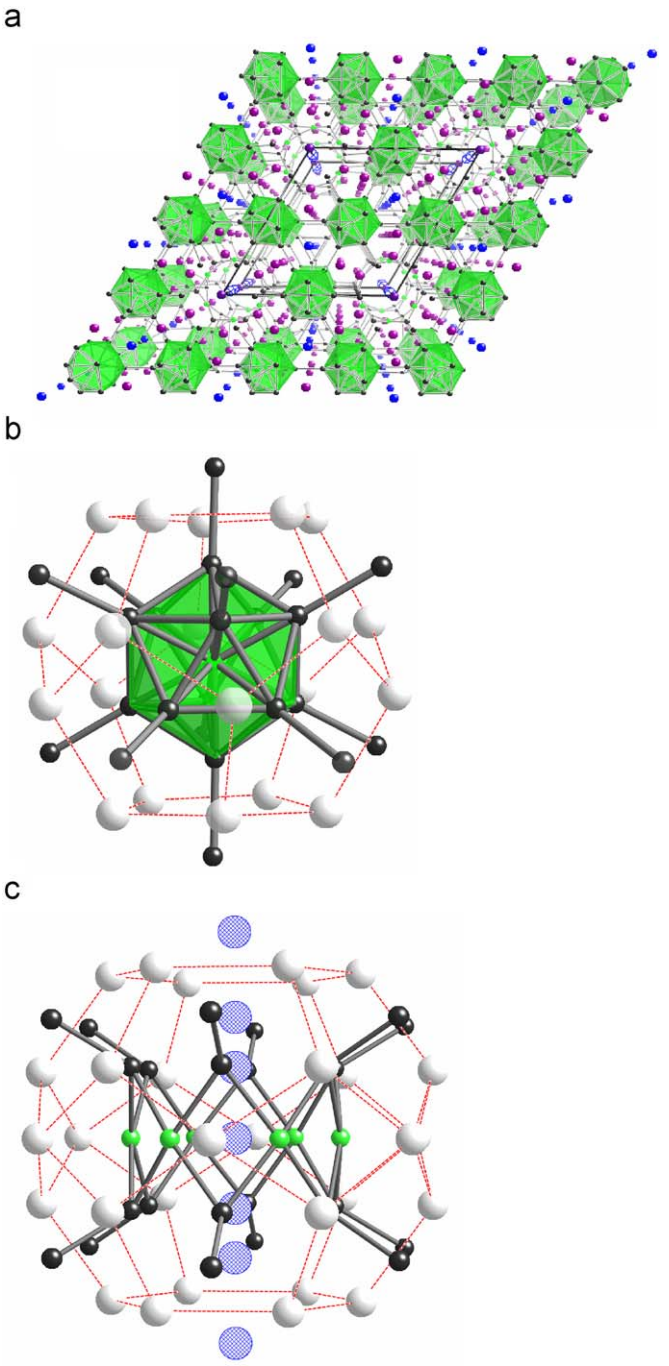

Fig. 6. The structure of $Yb_{6.7+x}Ca_{24.7-y}Ni_9Zn_{54}$: (a) the full structure viewed down the *c* axis, with $Ni@Zn_{12}$ icosahedra depicted in green; (b) pentagonal dodecahedron formed from Ca/Yb sites, centered by $Ni@Zn_{12}$ icosahedron; a similar building block is found in $Ca_{21}Ni_2Zn_{36}$; and (c) hexagonal symmetry cage formed from Ca/Yb sites, centered by a Ni/Zn drum surrounding the Ca/Yb partially occupied mixed sites that run along the *c* axis. Similar Ni/Zn hexagonal drums are found in $CaNi_2Zn_3$. (For interpretation of the references to color in this figure legend, the reader is referred to the web version of this article.)

4. Conclusions

Europium can be substituted into calcium intermetallics during Ca/Zn flux syntheses. However, for the systems studied here, the solid solution range is limited and a different structure forms in the presence of increasing amounts of europium in the reaction. In the substituted phases, the low temperatures of flux synthesis may facilitate inhomogeneous distribution of the elements mixing on lattice sites. This is likely particularly problematic for complex structures with several sites being substituted. Additional difficulty may stem from the fact that substitution of a flux element was attempted. Nonetheless, compounds containing Ca/Eu mixed sites appear to show interesting magnetic properties whether the europium is clustered (producing ferromagnetic regions) or more evenly distributed across the crystal (resulting in spin glass behavior). Different synthesis and processing techniques such as annealing will be investigated to see how the magnetic properties are affected.

Acknowledgments

This research made use of the Scanning Electron Microscope facilities of MARTECH at Florida State University. Financial support from the NSF (Grant DMR-05-47791) is gratefully acknowledged.

Appendix A. Supplementary material

Supplementary data associated with this article can be found in the online version at 10.1016/j.jssc.2009.06.001.

References

[1] [a] Z. Fisk, J.P. Remeika, in: Gschneider, Eyring (Eds.), Handbook on the Physics and Chemistry of Rare Earths, vol. 12, Elsevier Science, Amsterdam, 1989 (Chapter 81);
[b] Z. Fisk, P.C. Canfield, Philos. Mag. 65 (1992) 1117–1123.
[2] D. Elwell, H.J. Scheel, in: Crystal Growth from High-Temperature Solutions, Academic Press, Inc., London, 1975.
[3] M.G. Kanatzidis, R. Pöttgen, W. Jeitschko, Angew. Chem. Int. Ed. 44 (2005) 6996–7023.
[4] M. Stojanovic, S.E. Latturner, J. Solid State Chem. 180 (2007) 907–914.
[5] D. Lide, CRC Handbook of Chemistry and Physics, eighty eighth ed., CRC Press, Boca Raton, 2007.
[6] S.E. Latturner, D. Bilc, S.D. Mahanti, M.G. Kanatzidis, Inorg. Chem. 48 (2009) 1346–1355.
[7] A. Szytula, J. Leciejewicz, in: CRC Handbook of Crystal Structures and Magnetic Properties of Rare Earth Intermetallics, CRC Press, Boca Raton, 1994.
[8] [a] R. Mishra, R. Pöttgen, R.D. Hoffmann, D. Kaczorowski, H. Piotrowski, P. Mayer, C. Rosenhahn, B.D. Mosel, Z. Anorg. Allg. Chem. 627 (2001) 1283–1291;
[b] R.D. Hoffmann, R. Pöttgen, C. Rosenhahn, B.D. Mosel, B. Kunnen, G. Kotzyba, J. Solid State Chem. 145 (1999) 283–290.
[9] [a] SAINT, Version 6.02a, Bruker AXS, Inc., Madison, WI, 2000;
[b] G.M. Sheldrick, SHELXTL NT/2000, Version 6.1, Bruker AXS, Inc., Madison, WI, 2000.
[10] H.H. Hill, in: W.N. Miner (Ed.), Plutonium and Other Actinides, AIME, New York, 1970.
[11] K.F. Cai, L.C. Zhang, Q. Lei, E. Muller, C. Stiewe, Cryst. Growth Des. 6 (2006) 1797–1800.
[12] C.L. Condron, S.M. Kauzlarich, F. Gascoin, G.J. Snyder, Chem. Mater. 18 (2006) 4939–4945.
[13] E. Quarez, K.F. Hsu, R. Pcionek, N. Frangis, E.K. Polychroniadis, M.G. Kanatzidis, J. Am. Chem. Soc. 127 (2005) 9177–9190.
[14] [a] S. Serio, J.C. Waerenborgh, M. Almeida, M.M. Cruz, M. Godinho, J. Magn. Magn. Mater 272–276 (2004) e1947–e1948;
[b] S. Serio, L.C.J. Pereiera, M.M. Cruz, M. Godinho, J.C. Waerenborgh, J. Alloys Compd. 454 (2008) 16–23;
[c] A.P. Goncalves, L.C.J. Pereiera, J.C. Waerenborgh, D.P. Rojas, M. Almeida, L. Havela, H. Noel, Physica B 373 (2006) 8–15.
[15] S. Bobev, S.C. Sevov, Inorg. Chem. 39 (2000) 5930–5937.
[16] S. Bobev, S.C. Sevov, J. Solid State Chem. 153 (2000) 90.
[17] J.A. Mydosh, in: Spin Glasses: An Experimental Introduction, Taylor and Francis, London, 1993.
[18] [a] P. Villars, L.D. Calvert, Pearson's Handbook—Crystallographic Data for Intermetallic Phases, ASM International, Materials Park, OH, 1998;
[b] O.S. Zarechnyuk, N.B. Manyako, T.I. Yanson, V.A. Bruskov, Krystallografiya 33 (1988) 336–340.